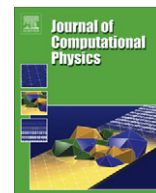




ELSEVIER

Contents lists available at ScienceDirect

## Journal of Computational Physics

journal homepage: [www.elsevier.com/locate/jcp](http://www.elsevier.com/locate/jcp)

# Efficient enforcement of far-field boundary conditions in the Transformed Field Expansions method

David P. Nicholls

*Department of Mathematics, Statistics, and Computer Science, University of Illinois at Chicago, Chicago, IL 60607, United States*

## ARTICLE INFO

*Article history:*

Received 14 September 2010

Received in revised form 25 May 2011

Accepted 25 July 2011

Available online xxxx

*Keywords:*

Dirichlet–Neumann operators

Boundary Perturbation Methods

Artificial Boundaries

Transparent Boundary Conditions

High-order/spectral methods

Legendre Spectral Element Methods

Water waves

## ABSTRACT

The Method of Transformed Field Expansions (TFE) has been demonstrated to be a robust and highly accurate numerical scheme for simulating solutions of boundary value and free boundary problems from the sciences and engineering. As a Boundary Perturbation Method it builds highly accurate solutions based upon exact solutions in a simple, canonical, geometry and corrects these via Taylor series to fit the actual geometry at hand. The TFE method has significantly enhanced stability properties when compared with other Boundary Perturbation approaches, however, this comes at the cost of requiring a full volumetric discretization as opposed to the surface formulation that other methods can realize. In this paper we outline two techniques for ameliorating this shortcoming, first by employing a Legendre Spectral Element Method to implement efficient, graded meshes, and second by utilizing an Artificial Boundary with a Transparent Boundary Condition placed quite close to the boundary of the domain. In this contribution we focus on the specific problem of simulating the Dirichlet–Neumann operator associated to Laplace's equation on a periodic cell (which arises in the water wave problem). While the details of our results are specific to this problem, the general conclusions are valid for the wider class of problems to which the TFE method can be applied. For each technique we discuss implementation details and display numerical results which support the conclusion that each of these techniques can greatly reduce the computational cost of using the TFE method.

© 2011 Elsevier Inc. All rights reserved.

## 1. Introduction

Boundary value and free boundary problems arise in all areas of the sciences and engineering, from fluid mechanics (e.g., water waves and Hele–Shaw flows [1]) to solid mechanics (e.g., Stefan problems, crystal growth [2]) to acoustics and electromagnetics [3]. In many cases the irregular domain shape is a relatively small perturbation of a much simpler (e.g., separable) geometry, which suggests that a perturbative technique is a profitable line of inquiry in such problems. Boundary Perturbation Methods (BPM) are precisely such a class of methods and have been shown to be accurate and reliable within their domain of applicability [4–6].

A shortcoming of some classical formulations is their subtle dependence upon significant cancellations to ensure their convergence [7–9] and, in response to this, the author (in collaboration with F. Reitich) devised a new stabilized approach dubbed the Method of Transformed Field Expansions (TFE) [7–9]. This approach not only delivered a simple and rigorous proof of analyticity properties which justify the necessary perturbation expansions, but also provided a stable and high-order algorithm for the computation of field and surface quantities of interest.

*E-mail address:* [nicholls@math.uic.edu](mailto:nicholls@math.uic.edu)

However, the enhanced stability of the TFE method comes at the cost of requiring a full volumetric discretization of the problem domain in contrast to other popular BPM which simply demand a *surface* discretization. Clearly, for problems with large domains this cost can be prohibitive and renders the TFE approach completely non-competitive. The point of this contribution is to outline two methods for ameliorating the costs associated with this discretization thereby rendering the TFE method a viable alternative. In this contribution we focus on the specific problem of simulating the Dirichlet–Neumann operator associated to Laplace’s equation on a periodic cell (which arises in the water wave problem). While the details of our results are specific to this problem, the general conclusions are valid for the wider class of problems to which the TFE method can be applied [10–17].

The first involves a fortuitous and sparse distribution of a *small* number of discretization points based upon *a priori* knowledge of the exact solution. For instance, solutions of Laplace’s equation are known to decay exponentially fast in the distance away from the boundary. This suggests that a Finite Element Method featuring elements which become exponentially large away from the boundary should be able to effectively capture the features of the solution while keeping the total number of problem unknowns quite low. In the first part of this paper we follow this line of inquiry almost exactly, save to utilize a Legendre Spectral Element Method (SEM) [18] in place of a generic *h*- or *p*-Finite Element Method to take advantage of the high accuracy which these SEM can achieve in regions of smoothness of the solution.

The second idea is an approach which has already been introduced to this problem [19,10,11] and has been used successfully in a number of other applications, particularly electromagnetics and linear acoustics [20–26]. In short we introduce an “artificial” boundary between the surface and the furthest extent of the domain and enforce an appropriate boundary condition there. Clearly, if the Artificial Boundary (AB) is chosen quite close to the surface of the domain, and if a “Transparent Boundary Condition” (which enforces an *exact* condition) is specified there, then this can be an enormously beneficial domain decomposition. In fact we find that such a boundary can be introduced, and the required exact boundary condition fits naturally into our spectral formulation. The question we address here is how close can the AB be brought to the surface of the domain without a significant loss of accuracy. As we shall show, the AB can generically be brought *almost* to the point of touching the domain boundary, while in the special case of a small boundary deformation it can be quite remarkably specified *beyond* the point of cavitation.

The organization of the paper is as follows: In Section 2 we recall the governing equations of the motion of the free-surface of an ideal fluid under the influence of gravity on a deep ocean and the role that Dirichlet–Neumann operators can play in a surface formulation. In Section 3 we recall some of the basic facts concerning the class of Boundary Perturbation Methods, specifically the Method of Transformed Field Expansions (Section 3.1) which we examine here in detail. In Section 4 we detail our Legendre Spectral Element Method and outline how it can be used to solve large-domain boundary value problems very efficiently; results of numerical experiments versus an exact solution (given in Section 4.1) are presented in Section 4.2. In Section 5 we discuss our Artificial Boundary approach for domain truncation to address the same problem. Again, numerical results are given in Section 5.1. Finally, a discussion of other approaches is presented in Section 5.2, and concluding remarks are given in Section 6.

## 2. Governing equations

A physically motivated problem which clearly demonstrates the need for efficient enforcement of far-field boundary conditions is the water wave problem on a deep ocean. We focus our attention on one of the central difficulties of the analytical and numerical simulation of this model, the task of computing the Dirichlet–Neumann operator (DNO) which we introduce below. As we shall see, this operator encodes *all* of the depth dependent effects and is therefore, for our present purposes, the only quantity of interest.

The Euler equations of free-surface ideal fluid flow constitute a highly accurate model for the evolution of a large body of water (e.g., an ocean or lake) under the influence of gravity. To be more precise, consider the domain

$$S_{h,\eta} := \{(x, y) \in \mathbf{R}^{d-1} \times \mathbf{R} \mid h < y < \eta(x, t)\},$$

where  $h$  is the mean fluid depth,  $d = 2, 3$  is the problem dimension, and  $\eta$  is the shape of the free surface deformation from the rest state  $y = 0$ . The equations of motion are [1]

$$\Delta\varphi = 0 \quad \text{in } S_{h,\eta}, \tag{1a}$$

$$\partial_y\varphi = 0 \quad \text{at } y = -h, \tag{1b}$$

$$\partial_t\eta - \partial_y\varphi + \nabla_x\eta \cdot \nabla_x\varphi = 0 \quad \text{at } y = \eta, \tag{1c}$$

$$\partial_t\varphi + g\eta + \frac{1}{2}|\nabla\varphi|^2 = 0 \quad \text{at } y = \eta, \tag{1d}$$

where  $\varphi$  is the velocity potential (the velocity is given by  $\vec{u} = \nabla\varphi$ ) and  $g$  is the gravitational constant. In the lateral direction we specify the classical periodic boundary conditions,

$$\varphi(x + \gamma, y, t) = \varphi(x, y, t), \quad \eta(x + \gamma, t) = \eta(x, t), \quad \forall \gamma \in \Gamma,$$

where  $\Gamma$  is a lattice in  $\mathbf{R}^{d-1}$ . This lattice  $\Gamma$  generates a conjugate lattice  $\Gamma'$  of wavenumbers (e.g., if  $\Gamma = L\mathbf{Z} \times M\mathbf{Z}$  then  $\Gamma' = (2\pi/L)\mathbf{Z} \times (2\pi/M)\mathbf{Z}$ ). In terms of this notation we can express the Fourier series of a function as

$$f(x) = \sum_{k \in \Gamma'} \hat{f}_k e^{ik \cdot x},$$

where  $\hat{f}_k$  is the  $k$ -th Fourier coefficient of  $f$ .

Zakharov [27] restated the problem (1) as a Hamiltonian system with the surface quantities  $\eta(x,t)$  and  $\xi(x,t) := \varphi(x, \eta(x,t), t)$  as the canonical variables. Craig and Sulem [5] made this characterization much more explicit with the introduction of the DNO. To define the DNO, consider the rather generic elliptic problem inspired by (1)

$$\Delta v = 0 \text{ in } S_{h,\sigma}, \quad (2a)$$

$$v(x, \sigma(x)) = \xi(x), \quad (2b)$$

$$\partial_y v(x, -h) = 0, \quad (2c)$$

$$v(x + \gamma, y) = v(x, y) \quad \forall \gamma \in \Gamma, \quad (2d)$$

where  $v$  is to be determined from given boundary shape  $\sigma$  and Dirichlet data  $\xi$ . Provided that  $\sigma$  is sufficiently smooth (2) will have a unique solution [28,29] whose normal derivative,  $v(x)$ , can be computed at the surface  $y = \sigma$ . This mapping,  $G$ , of the Dirichlet data  $\xi$  to Neumann data  $v$  is precisely the DNO:

$$G(\sigma)[\xi] := [\nabla v]_{y=\sigma} \cdot N = \partial_y v(x, \sigma(x)) - \nabla_x \sigma \cdot \nabla_x v(x, \sigma(x)), \quad (3)$$

where  $N = (1, -\nabla_x \sigma)^T$  is an exterior normal. Given this definition of the DNO, a straightforward application of the chain rule transforms (1) to

$$\partial_t \eta = G(\eta)[\xi], \quad (4a)$$

$$\begin{aligned} \partial_t \xi = & -g\eta - \frac{1}{2(1 + |\nabla_x \eta|^2)} \left[ |\nabla_x \xi|^2 - (G(\eta)[\xi])^2 \right. \\ & \left. - 2(\nabla_x \xi \cdot \nabla_x \eta)G(\eta)[\xi] + |\nabla_x \xi|^2 |\nabla_x \eta|^2 - (\nabla_x \xi \cdot \nabla_x \eta)^2 \right], \end{aligned} \quad (4b)$$

c.f. [5].

### 3. Boundary Perturbations

Having restated the Euler Eq. (1) in terms of surface variables (4) via the specification of Zakharov [27] and Craig and Sulem [5], a critical numerical concern is the robust computation of the DNO. As we stated in the Introduction, if the surface deformation,  $\sigma(x)$ , is not too large then a perturbative method is natural and, as we shall see, can deliver highly accurate solutions in a robust fashion. With this philosophy in mind several Boundary Perturbation Methods (BPM) have been devised to compute the DNO (or equivalent operators) including the method of ‘‘Operator Expansions’’ (OE) [30,4,31–33,5,34–39], the method of ‘‘Field Expansions’’ (FE) [6,40–45], and the Method of ‘‘Transformed Field Expansions’’ (TFE) [7–9,19,10]. While the two former methods can be shown to be highly accurate within their domain of applicability with extremely favorable operation counts (typically the fastest known for the problem in question), they have each been shown to be *unstable* for many geometries of applied interest. More specifically, if the surface shape,  $\sigma(x)$ , is large and/or rough, thereby requiring a large number of terms in the underlying perturbation expansions, subtle cancellations present in the OE and FE formulations become evident and (otherwise negligible) round-off errors are magnified to order one and larger [7,9,19].

In [7] the author and Reitich devised the TFE approach, which we study in this publication, to remedy these instabilities. This effort was completely successful and delivers a method which is not only highly accurate (spectrally accurate if  $\sigma(x)$  is analytic) but also stable and robust. The one trade-off for this enhanced stability is that the TFE method requires a discretization of the *depth* variable (e.g., the  $y$ -coordinate in (2) above) whereas the OE and FE approaches are *surface* methods (requiring only a lateral discretization). It is precisely this issue which we address in this contribution posed as two specific questions:

1. If the vertical dimension is large (i.e.,  $h \gg 1$ ) can the known structure of the solution be used to partition this dimension so that a solution can be rapidly computed?
2. Can the computational domain be significantly truncated with an ‘‘Artificial Boundary’’ (AB) to reduce the computational cost while retaining the fidelity of the solution? If this can be accomplished how close can the AB be brought to the surface of the domain?

Before addressing these questions we recall the TFE method.

#### 3.1. Transformed Field Expansions

The theorems of Calderón [46], Coifman and Meyer [47], Craig et al. [37], and Nicholls and Reitich [7] demonstrate that the DNO is analytic with respect to boundary perturbations so that if  $\sigma(x) = \varepsilon f(x)$ , the expansion

$$G(\sigma)[\xi] = G(\varepsilon f)[\xi] = \sum_{n=0}^{\infty} G_n(f)[\xi] \varepsilon^n, \quad (5)$$

converges strongly in an appropriate Sobolev space if  $f$  is sufficiently smooth. The TFE recursions find convenient formulas for the  $G_n$  which can then be used to find highly accurate approximations of the DNO via

$$G^N(\varepsilon f)[\xi] := \sum_{n=0}^N G_n(f)[\xi] \varepsilon^n. \quad (6)$$

The TFE method for (2) begins with a change of variables

$$x' = x, \quad y' = h \left( \frac{y - \sigma(x)}{h + \sigma(x)} \right), \quad (7)$$

which transforms the domain  $S_{h,\sigma}$  to  $S_{h,0}$ . Given (2) and (7), the transformed field quantity

$$u(x', y') := v \left( x', \frac{y'(h + \sigma(x'))}{h} + \sigma(x') \right),$$

satisfies, upon dropping primes,

$$\Delta u = F(x, y; \sigma, u, h) \quad \text{in } S_{h,0}, \quad (8a)$$

$$u(x, 0) = \xi(x), \quad (8b)$$

$$\partial_y u(x, -h) = 0, \quad (8c)$$

$$u(x + \gamma, y) = u(x, y) \quad \forall \gamma \in \Gamma, \quad (8d)$$

where

$$F = \operatorname{div}_x [F_x] + \partial_y F_y + F_0. \quad (8e)$$

The  $x$ -derivative,  $y$ -derivative, and homogeneous parts of  $F$  are given by:

$$F_x = -\frac{2}{h} \sigma \nabla_x u - \frac{1}{h^2} \sigma^2 \nabla_x u + \frac{h+y}{h} \nabla_x \sigma \partial_y u + \frac{h+y}{h^2} \sigma \nabla_x \sigma \partial_y u, \quad (8f)$$

$$F_y = \frac{h+y}{h} \nabla_x \sigma \cdot \nabla_x u + \frac{h+y}{h^2} \sigma \nabla_x \sigma \cdot \nabla_x u - \frac{(h+y)^2}{h^2} |\nabla_x \sigma|^2 \partial_y u, \quad (8g)$$

and

$$F_0 = \frac{1}{h} \nabla_x \sigma \cdot \nabla_x u + \frac{1}{h^2} \sigma \nabla_x \sigma \cdot \nabla_x u - \frac{h+y}{h^2} |\nabla_x \sigma|^2 \partial_y u. \quad (8h)$$

Additionally, the DNO transforms to

$$G(\sigma)[\xi] = \partial_y u(x, 0) + H(x; \sigma, u, h), \quad (9a)$$

where

$$H = -\frac{1}{h} \sigma G(\sigma)[\xi] - \nabla_x \sigma \cdot \nabla_x u(x, 0) - \frac{1}{h} \sigma \nabla_x \sigma \cdot \nabla_x u(x, 0) + |\nabla_x \sigma|^2 \partial_y u(x, 0), \quad (9b)$$

c.f. [7]. The important fact about this particular gathering of terms is that  $F$  and  $H$  are  $\mathcal{O}(\sigma)$ .

With (8) and (9) in hand, if we set  $\sigma(x) = \varepsilon f(x)$ , the TFE method now instructs us to make the following Taylor series expansions for the field and DNO

$$u(x, y; \varepsilon) = \sum_{n=0}^{\infty} u_n(x, y) \varepsilon^n, \quad G(\varepsilon f)[\xi] = \sum_{n=0}^{\infty} G_n(f)[\xi] \varepsilon^n. \quad (10)$$

Upon insertion of (10) into (8), we find that the  $u_n$  must satisfy

$$\Delta u_n = F_n(x, y; h) \quad \text{in } S_{h,0}, \quad (11a)$$

$$u_n(x, 0) = \delta_{n,0} \xi(x), \quad (11b)$$

$$\partial_y u_n(x, -h) = 0, \quad (11c)$$

$$u_n(x + \gamma, y) = u_n(x, y) \quad \forall \gamma \in \Gamma, \quad (11d)$$

where  $\delta_{n,m}$  is the Kronecker delta,

$$F_n = \text{div}_x[F_{x,n}] + \partial_y F_{y,n} + F_{0,n}, \quad (11e)$$

$$F_{x,n} = -\frac{2}{h}f\nabla_x u_{n-1} - \frac{1}{h^2}f^2\nabla_x u_{n-2} + \frac{h+y}{h}\nabla_x f\partial_y u_{n-1} + \frac{h+y}{h^2}f\nabla_x f\partial_y u_{n-2}, \quad (11f)$$

$$F_{y,n} = \frac{h+y}{h}\nabla_x f \cdot \nabla_x u_{n-1} + \frac{h+y}{h^2}f\nabla_x f \cdot \nabla_x u_{n-2} - \frac{(h+y)^2}{h^2}|\nabla_x f|^2\partial_y u_{n-2}, \quad (11g)$$

and

$$F_{0,n} = \frac{1}{h}\nabla_x f \cdot \nabla_x u_{n-1} + \frac{1}{h^2}f\nabla_x f \cdot \nabla_x u_{n-2} - \frac{h+y}{h^2}|\nabla_x f|^2\partial_y u_{n-2}. \quad (11h)$$

In these and future formulas any function with a negative index should be replaced by zero. Furthermore, the expansion of  $G$  (10), inserted into (9) yields

$$G_n(f)(\xi) = \partial_y u_n(x, 0) + H_n(x; h), \quad (12a)$$

where

$$H_n = -\frac{1}{h}fG_{n-1}(f)(\xi) - \nabla_x f \cdot \nabla_x u_{n-1}(x, 0) - \frac{1}{h}f\nabla_x f \cdot \nabla_x u_{n-2}(x, 0) + |\nabla_x f|^2\partial_y u_{n-2}(x, 0), \quad (12b)$$

see [7].

#### 4. A Legendre Spectral Element Method for TFE

At this point we are in a position to specify precisely how we will numerically approximate the DNO. For the numerical implementation of our TFE method we follow the high-order/spectral philosophy of Nicholls and Reitich [8]. As we remarked earlier, we will approximate the DNO,  $G$ , by the truncated Taylor series (6), and for simplicity we will focus on the  $d = 2$  dimensional problem and set the period of our profiles to be  $L = 2\pi$ . As we saw, to compute the DNO the TFE procedure requires first the simulation of the Taylor orders of the field,  $u_n$ , before the  $G_n$  can be approximated.

Beginning with the elliptic problem satisfied by  $u_n$ , (11), we note that the periodic boundary conditions mandate that

$$u_n(x, y) = \sum_{k=-\infty}^{\infty} \hat{u}_{n,k}(y)e^{ikx},$$

while the remaining three equations translate to the following two-point boundary value problem for  $\hat{u}_{n,k}$ :

$$\partial_y^2 \hat{u}_{n,k}(y) - |k|^2 \hat{u}_{n,k}(y) = \hat{F}_{n,k}(y; h) \quad -h < y < 0, \quad (13a)$$

$$\hat{u}_{n,k}(0) = \delta_{n,0} \hat{\xi}_k, \quad (13b)$$

$$\partial_y \hat{u}_{n,k}(-h) = 0. \quad (13c)$$

We now have a wide array of numerical methods and philosophies at our disposal to simulate solutions of (13). In our previous work [7,8] we advocated a classical Chebyshev tau approach [48] which seeks approximate solutions of the form

$$\hat{u}_{n,k}^{N_y} := \sum_{l=0}^{N_y} \hat{u}_{n,k,l} T_l\left(\frac{2y+h}{h}\right), \quad (14)$$

where  $T_l$  is the  $l$ th Chebyshev polynomial, and the coefficients  $\hat{u}_{n,k,l}$  are chosen so that the boundary conditions are satisfied *exactly*. There are  $(N_y - 1)$  – many more conditions realized by inserting the form (14) into (13a) and equating at like polynomial orders. This generates a dense system of linear equations to be solved which would generically require  $\mathcal{O}(N_y^3)$  operations. However, as described in [48], the bulk of these can be cleverly recombined to give a pentadiagonal system with dense sub-blocks associated to the (two) boundary conditions. When combined with the availability of the  $\mathcal{O}(N_y \log(N_y))$  fast Chebyshev transform (realized via the Fast Fourier Transform algorithm [48]), the entire system of equations can be solved very rapidly in  $\mathcal{O}(N_y \log(N_y))$  operations. This approach has been a wildly successful cog in the TFE framework to the point that one may wonder if any other approaches need be considered.

However, one weakness of the Chebyshev tau method described above is its *global* nature: The entire domain  $[-h, 0]$  is discretized simultaneously. The fortuitous choice of Chebyshev basis functions typically ensures that the “minimal” number of coefficients  $\hat{u}_{n,k,l}$  need be chosen, however, as the size of the domain increases,  $N_y$  *must* increase as well. It is an inevitability that for a large enough domain, an approach with some type of local character will give superior performance. With this in mind we introduce the Legendre Spectral Element Method (SEM) below.

As it is quite clearly explained in Section 2.4 of [18], the SEM shares many characteristics with classic Galerkin  $h$ - and  $p$ -Finite Element Methods (FEM). Among these, for the  $h$ -version, a partition of the domain into elements, e.g.,

$$[-h, 0] = \bigcup_{e=1}^E [a_e, b_e].$$

Lagrangian interpolation formulas on each element, and basis functions which have *local* support. In similarity with  $p$ -version FEM, high-order polynomials are used as local basis functions to take advantage of high accuracy for smooth solutions. As [18] point out, SEM have the additional feature that, due to the use of Gaussian quadrature, the sparseness of discretization operators is due not only to the local support of the basis functions, but also the integration rules utilized.

To summarize the developments of [18] for an application of an SEM to the boundary value problem (13a), the differential equation must be posed weakly via integration by parts with the Dirichlet condition imposed essentially while the Robin condition is enforced naturally. Each element  $[a_e, b_e]$  is mapped to the reference domain  $[-1, 1]$  and the approximate solution expressed there in terms of Lagrange interpolation polynomials,  $\pi_l(s)$ , based upon the Gauss–Lobatto–Legendre (GLL) points

$$u_N^e(s) = \sum_{l=0}^{N_y} u_l^e \pi_l(s), \quad s \in [-1, 1]$$

(which include the endpoints so that continuity can be *explicitly* enforced). Local mass and stiffness matrices are easily constructed and assembled into global mass and stiffness matrices using well-known FEM technology. SEM possess many features which make them particularly appealing for BVP with smooth solutions including mass and stiffness matrices with sparseness properties which are easy to exploit, high order accuracy, and the ability to adaptively refine in both polynomial order ( $p$ -refinement) and spatial discretization ( $h$ -refinement). It is this latter property that we exploit here.

To begin we point out that solutions of (13a) and (2) decay exponentially fast as  $y$  decreases to negative infinity. In the case of a flat interface ( $\sigma(x) \equiv 0$ ) this can be seen directly from the exact solution

$$v_0(x, y) = \sum_{k=-\infty}^{\infty} \zeta_k \frac{\cosh(|k|(y+h))}{\cosh(|k|h)} e^{ikx},$$

and for more general geometries this is a well-known property of solutions of Laplace's equation [29]. So, in the case that  $h$  is large (but finite), an equally spaced partition of  $[-h, 0]$  is clearly very wasteful as the solution is nearly constant (zero) over most of the partition. A much more efficient idea is to distribute the partition endpoints *exponentially* to match the behavior of the exact solution (away from the boundary), and this is precisely the approach we advocate here.

To be specific, in the global (single element) ‘‘Chebyshev tau method’’ we approximate the transformed field  $u(x, y)$  by

$$u_{Cheby}^{N, N_x, N_y}(x, y) := \sum_{n=0}^N \sum_{k=-N_x/2}^{N_x/2-1} \sum_{l=0}^{N_y} \hat{u}_{n,k,l} T_l\left(\frac{2y+h}{h}\right) e^{ikx} \varepsilon^n. \quad (15)$$

In the local (multi-element) ‘‘Legendre SEM’’ we approximate  $u(x, y)$  by

$$u_{Leg}^{N, N_x, N_y, E}(x, y) := \sum_{n=0}^N \sum_{k=-N_x/2}^{N_x/2-1} \sum_{l=0}^{N_y} \sum_{e=1}^E \tilde{u}_{n,k,l,e} \pi_l(s_e) e^{ikx} \varepsilon^n, \quad (16)$$

where  $s_e$  is in the reference interval  $[-1, 1]$  after having been mapped from  $[a_e, b_e]$ . In either case, once the  $u$  are approximated,  $G$  can be simulated by

$$G^{N, N_x} := \sum_{n=0}^N \sum_{k=-N_x/2}^{N_x/2-1} \hat{G}_{n,k} e^{ikx} \varepsilon^n, \quad (17)$$

and (12).

#### 4.1. Exact solutions

In the case of non-trivial interface shape,  $y = \sigma(x)$ , there are no known exact solutions of (2). To carry out a convergence study for our algorithm to compute the DNO, we utilize the following principle: In building a numerical solver for the homogeneous PDE and boundary conditions:

$$\begin{aligned} \mathcal{L}u &= 0 & \text{in } \Omega, \\ \mathcal{B}u &= 0 & \text{at } \partial\Omega, \end{aligned}$$

it is often, as it is here, no more difficult to construct an algorithm for the corresponding inhomogeneous problem:

$$\begin{aligned} \mathcal{L}u &= \mathcal{R} & \text{in } \Omega, \\ \mathcal{B}u &= \mathcal{Q} & \text{at } \partial\Omega. \end{aligned}$$

Selecting an arbitrary function  $w$ , we can compute

$$\mathcal{R}_w := \mathcal{L}w, \quad \mathcal{Q}_w := \mathcal{B}w,$$

and now have an *exact* solution to the problem

$$\begin{aligned}\mathcal{L}u &= \mathcal{R}_w \quad \text{in } \Omega \\ \mathcal{B}u &= \mathcal{Q}_w \quad \text{at } \partial\Omega,\end{aligned}$$

namely  $u = w$ . In this way we can rigorously test our inhomogeneous solver for which the homogeneous solver is a special case. However, one does need to be careful to consider  $w$  which have the same “behavior” as solutions  $u$  of the inhomogeneous problem and here we find  $w$  such that  $\mathcal{R}_w \equiv 0$ .

For the exact solution consider the function

$$u_p(x, y) := \frac{\cosh(|p|(y+h))}{\cosh(|p|h)} e^{ipx}, \quad p \in \mathbf{Z},$$

which satisfies (2a), (2c) and (2d) (i.e.  $\mathcal{R}_w \equiv 0$  in the language above). If we now choose a boundary deformation  $\sigma(x)$  we can specify Dirichlet data

$$\xi_p(x) := \frac{\cosh(|p|(\sigma+h))}{\cosh(|p|h)} e^{ipx},$$

(i.e.  $\mathcal{Q}_w$ ) which has the *exact* Neumann data:

$$v_p(x) := (\partial_y u_p - (\partial_x \sigma) \partial_x u_p)_{y=\sigma(x)} = \left\{ |p| \frac{\sinh(|p|(\sigma+h))}{\cosh(|p|h)} - (\partial_x \sigma)(ip) \frac{\cosh(|p|(\sigma+h))}{\cosh(|p|h)} \right\} e^{ipx}.$$

With this  $\{\xi_p, v_p\}$  pair (we will always select  $p = 2$  in this contribution) it is now easy to test the convergence of simulations of the DNO.

#### 4.2. Numerical results: Legendre SEM

To assess the utility of our new approach we present numerical simulations compared to these specially constructed exact solutions which provide, for given Dirichlet data, the corresponding exact Neumann data. We test these numerical methods for surface deformations,  $\sigma = \varepsilon f$ , of varying sizes  $\varepsilon$  for the fixed, large, depth  $h = 1000$ . We show how the new Legendre SEM can be used to great effect to reduce the computational effort of the TFE approach without sacrificing accuracy or stability.

To fix upon a particular problem we consider the problem of simulating the DNO on a domain of (nondimensional) length  $L = 2\pi$  and depth  $h = 1000$ . We choose an *analytic* (sinusoidal) boundary deformation

$$\sigma(x) = \varepsilon f(x) = \varepsilon \cos(x),$$

to guarantee that the series (10) will converge extremely rapidly. To distribute the endpoints  $(a_e, b_e)$  we have chosen a simple exponential distribution where equally spaced points

$$y_m = m \left( \frac{(-h) - 0}{M} \right) = -\frac{mh}{M}, \quad m = 0, \dots, M,$$

are mapped to

$$\tilde{y}_m = 1 - e^{\eta|y_m|},$$

where we chose, rather arbitrarily,  $\eta = 0.03$  for the simulations presented here. Clearly, some (possibly many) of these are mapped *outside* the domain  $[-h, 0]$  and these are discarded. Regardless of the distribution of points, we always choose the endpoints  $y = 0, -h$  to enforce the boundary conditions explicitly. There is nothing special about the transformation we have chosen, and many others could be used and similar results realized.

To make an effective comparison of our new and old approaches we set ourselves the task of computing the DNO with accuracy  $10^{-10}$  in the fastest time possible. The computations were performed in C++ on the author’s dual quad-core Mac Pro desktop system, however, we nondimensionalize time (by the best time we could achieve with the Chebyshev tau method,  $T_C$ ) so that the results are “universal.”

To begin we considered the quite small perturbation amplitude  $\varepsilon = 0.01$ . For both the Chebyshev tau and Legendre SEM simulations we chose  $N_x = 32$  equally spaced gridpoints along the  $x$ -interval, and  $N = 4$  Taylor orders in the expansion of the field and DNO, both of which were sufficient to resolve these to machine precision. For the Chebyshev tau solver we were forced to choose  $N_y = 256$  to realize  $2.77 \times 10^{-10}$  accuracy; the average time for this simulation was  $T_C = 32.49$  s (over 10 runs). In Table 1 we summarize results of our Legendre SEM with varying choices of  $N_y$  and  $E$  with times scaled to the average Chebyshev cost (32.49 s). From this data it is easy to see that we can realize five-fold savings by using our unequally spaced Legendre SEM versus our old Chebyshev tau method without *any* degradation in the accuracy attained.

To further test these conclusions we present in Tables 2 and 3 the results of computations with the value of  $\varepsilon$  raised to the more challenging values of 0.1 and 0.5, respectively. For consistency (and to keep the computation times as reasonable as possible) we have fixed the number of gridpoints used by the Chebyshev tau method at  $N_y = 256$  and chosen as our “target

**Table 1**

Numerical parameters, relative errors, and average timings (over 10 samples) for Legendre SEM simulation of the DNO with  $\varepsilon = 0.01$ ,  $h = 1000$ , and  $L = 2\pi$ . The average times are nondimensionalized by the time,  $T_C = 32.49$  s, for a Chebyshev tau simulation with  $N_x = 32$ ,  $N_y = 256$ , and  $N = 4$ .

$N_x$	$N_y$	$E$	$N$	Relative error	Scaled average time
32	16	5	4	$1.30785 \times 10^{-10}$	0.2086
32	14	6	4	$2.00419 \times 10^{-10}$	0.1780
32	12	8	4	$6.30483 \times 10^{-11}$	0.1543
32	10	14	4	$1.50742 \times 10^{-11}$	0.1516
32	8	22	4	$1.29823 \times 10^{-10}$	0.1535
32	6	65	4	$1.87644 \times 10^{-10}$	0.3749

**Table 2**

Numerical parameters, relative errors, and average timings (over 10 samples) for Legendre SEM simulation of the DNO with  $\varepsilon = 0.1$ ,  $h = 1000$ , and  $L = 2\pi$ . The average times are nondimensionalized by the time,  $T_C = 91.3821$  s, for a Chebyshev tau simulation with  $N_x = 32$ ,  $N_y = 256$ , and  $N = 8$ .

$N_x$	$N_y$	$E$	$N$	Relative error	Scaled average time
32	16	5	8	$1.67436 \times 10^{-9}$	0.1772
32	14	6	8	$1.74445 \times 10^{-9}$	0.1502
32	12	8	8	$2.82997 \times 10^{-10}$	0.1310
32	10	14	8	$3.98266 \times 10^{-11}$	0.1314
32	8	22	8	$2.2048 \times 10^{-10}$	0.1341
32	6	65	8	$4.80333 \times 10^{-10}$	0.3153

**Table 3**

Numerical parameters, relative errors, and average timings (over 10 samples) for Legendre SEM simulation of the DNO with  $\varepsilon = 0.5$ ,  $h = 1000$ , and  $L = 2\pi$ . The average times are nondimensionalized by the time,  $T_C = 324.975$  s, for a Chebyshev tau simulation with  $N_x = 32$ ,  $N_y = 256$ , and  $N = 28$ .

$N_x$	$N_y$	$E$	$N$	Relative error	Scaled average time
32	16	5	28	$2.1256 \times 10^{-8}$	0.1778
32	14	6	28	$2.18663 \times 10^{-8}$	0.1511
32	12	8	28	$3.39867 \times 10^{-9}$	0.1315
32	10	14	28	$7.60097 \times 10^{-11}$	0.1301
32	8	22	28	$1.66424 \times 10^{-9}$	0.1332
32	6	65	28	$7.43621 \times 10^{-9}$	0.3125

error tolerance” the relative error realized by the Chebyshev method ( $10^{-9}$  with  $N = 8$  for  $\varepsilon = 0.1$ , and  $10^{-9}$  for  $N = 28$  for  $\varepsilon = 0.5$ ). This resulted in reference times  $T_C = 91.3821$  s and  $T_C = 324.975$  s, respectively. These data indicate that our new method behaves very much as it does in the  $\varepsilon = 0.01$  case, enabling five- to seven-fold reductions in computational time over the Chebyshev tau method.

**Remark 1.** Before closing this section we mention that the TFE method we describe here is, by no means, the only BP method which could be brought to bear on this problem. For instance, the Field Expansions (FE) method of Bruno and Reitich [6] can be applied and, for sake of comparison, we now report averaged computing times for this algorithm applied to the three computations above.

In the case  $\varepsilon = 0.01$  we can realize errors on the order of  $10^{-10}$  with  $N_x = 32$  (no vertical discretization is required) and  $N = 4$  in scaled time  $1.9 \times 10^{-4}$ . This remarkable execution time (roughly 1000 times faster than our Legendre SEM) highlights the truly advantageous behavior of the FE approach within its domain of applicability. For  $\varepsilon = 0.1$  we repeat this experiment with  $N_x = 32$  and  $N = 8$  and find scaled time  $2.1 \times 10^{-4}$ , which is, once again, astonishingly fast.

Finally, we report on the case  $\varepsilon = 0.5$  with  $N = 28$ . Here, with  $N_x = 32$  we can only achieve error  $10^{-3}$ , and this requires numerical analytic continuation via Padé summation (Taylor summation gives no accuracy) [49,8]. With  $N_x = 64$  we obtain an error of  $10^{-7}$ , while with  $N_x = 128$  we get worse results,  $10^{-4}$ ; the catastrophic cancellation errors inherent to this method are beginning to emerge. A brief search of the parameter space indicates that the best error one can achieve is  $10^{-8}$ , thereby failing to meet our precision specification, with  $N_x = 46$  which wonderfully illustrates the necessity of utilizing the TFE approach.

## 5. Near-field Transparent Boundary Conditions for TFE

The advantageous redistribution of mesh endpoints is not the only way we can use knowledge of the far-field solution of (2) to approximate solutions more efficiently. In fact, an alternative approach has previously been used by the author for not



only this purpose, but also to impose boundary conditions at infinity (“far field”) at finite (“near field”) values [19,10,11]. The idea is to introduce an “Artificial Boundary” (AB) at a location *within* the domain  $S_{h,\sigma}$ , and impose a Transparent (exact) Boundary Condition there. Of course this approach will enable huge computational savings if the AB can be brought quite close to the interface  $y = \sigma(x)$  as very few unknowns will be required to resolve the field, and it is the goal of this section to study just how close this choice may be made.

Before beginning we note that this idea of imposing an exact boundary condition at an Artificial Boundary has been explored by a number of other authors for different numerical discretization methods. For instance, in connection with the Finite Element Method we quote the work of Feng [50], Han and Wu [20], Keller and Givoli [21–23], the surveys of Givoli [51,25], and our own work [52–54], and the references therein.

We recall the developments of [11] by considering a hyperplane  $y = -a$ , with  $-h < -a < -|\sigma|_{L^\infty}$ , for the Artificial Boundary. We augment our original generic elliptic problem (2) with compatibility conditions at  $y = -a$ :

$$\Delta v = 0 \quad \text{in } S_{a,\sigma}, \quad (18a)$$

$$v(x, \sigma(x)) = \xi(x), \quad (18b)$$

$$\Delta w = 0 \quad -h < y < -a, \quad (18c)$$

$$v(x, -a) = w(x, -a), \quad (18d)$$

$$\partial_y v(x, -a) = \partial_y w(x, -a), \quad (18e)$$

$$\partial_y w(x, -h) = 0, \quad (18f)$$

$$v(x + \gamma, y) = v(x, y) \quad \forall \gamma \in \Gamma, \quad (18g)$$

$$w(x + \gamma, y) = w(x, y) \quad \forall \gamma \in \Gamma, \quad (18h)$$

and note that solutions of (2) and (18) are equivalent, i.e.,  $v$  matches on  $S_{a,\sigma}$  and  $v = w$  on  $-h < y < -a$ . To state our Transparent Boundary Condition we note that the problem (18c), (18f), and (18h) has solution

$$w(x, y) = \sum_{k=-\infty}^{\infty} a_k \frac{\cosh(|k|(y+h))}{\cosh(|k|(h-a))} e^{ikx}. \quad (19)$$

Furthermore, if we denote the Dirichlet data  $w(x, -a)$ , provided in (18d), by the generic function  $\psi(x)$  then we can write (19) as

$$w(x, y) = \sum_{k=-\infty}^{\infty} \hat{\psi}_k \frac{\cosh(|k|(y+h))}{\cosh(|k|(h-a))} e^{ikx},$$

where  $\hat{\psi}_k$  are the Fourier coefficients of  $\psi(x)$ . Additionally, we can compute the DNO at the hyperplane  $y = -a$ ,  $T$ , by the formula

$$T[\psi] = \partial_y w(x, -a) = \sum_{k=-\infty}^{\infty} \hat{\psi}_k |k| \tanh(|k|(h-a)) e^{ikx}.$$

We can find a unique solution  $v(x, y)$  to the Eqs. (18a), (18b) and (18g) provided we can produce the normal derivative of  $v$  at  $y = -a$ . This is furnished by (18e) and the DNO  $T$ . Thus, our original elliptic problem (2) is *equivalent* to the following system posed on the *truncated* domain  $S_{a,\sigma}$ :

$$\Delta v = 0 \quad \text{in } S_{a,\sigma}, \quad (20a)$$

$$v(x, \sigma(x)) = \xi(x), \quad (20b)$$

$$\partial_y v(x, -a) - T[v(x, -a)] = 0, \quad (20c)$$

$$v(x + \gamma, y) = v(x, y) \quad \forall \gamma \in \Gamma. \quad (20d)$$

Our new approach to efficient calculation of Laplace’s equation on large ( $h \gg 1$ ) domains is now clear: Provided that one can compute  $T$  quickly and accurately, simply set the AB as close to the interface  $y = \sigma(x)$  as possible to minimize the number of discretization points  $N_y$  in the  $y$ -coordinate.

Following the developments of Section 3.1 we once again make a domain transforming change of variables

$$x' = x, \quad y' = a \left( \frac{y - \sigma(x)}{a + \sigma(x)} \right),$$

c.f. (7), resulting in an inhomogeneous problem similar to (8) for the transformed field

$$u(x', y') := v \left( x', \frac{y'(a + \sigma(x'))}{a} + \sigma(x') \right).$$

We spare the reader the details of the resulting problem (see [55,11]) save to note that in (8) and (9),  $h$  is replaced by  $a$  (e.g., the right hand side is  $F(x,y; \sigma, u, a)$ ), and (8c) more specifically changes, upon dropping primes, to

$$\partial_y u(x, -a) - T[u(x, -a)] = J(x; \sigma, u, a) := \frac{1}{a} \sigma T[u(x, -a)].$$

Again, upon setting  $\sigma(x) = \varepsilon f(x)$ , we expand the transformed field and DNO in Taylor series in  $\varepsilon$ , c.f. (10)

$$u(x, y; \varepsilon) = \sum_{n=0}^{\infty} u_n(x, y) \varepsilon^n, \quad G(\varepsilon f)[\xi] = \sum_{n=0}^{\infty} G_n(f)[\xi] \varepsilon^n,$$

and each of these  $\{u_n, G_n\}$  satisfy problems similar to (11) and (12). Once again  $h$  is simply replaced by  $a$  in (11) and (12) (e.g., the right hand side is replaced by  $F_n(x, y; a)$ ), while (11c) becomes

$$\partial_y u_n(x, -a) - T[u_n(x, -a)] = J_n(x) := \frac{1}{a} f T[u_{n-1}(x, -a)].$$

Assuming once again that  $d = 2$  and  $L = 2\pi$ , the periodic boundary conditions force the  $u_n$  to have the form

$$u_n(x, y) = \sum_{k=-\infty}^{\infty} \hat{u}_{n,k}(y) e^{ikx},$$

where the  $\hat{u}_{n,k}$  satisfy

$$\partial_y^2 \hat{u}_{n,k}(y) - |k|^2 \hat{u}_{n,k}(y) = \hat{F}_{n,k}(y; a) \quad -a < y < 0, \quad (21a)$$

$$\hat{u}_{n,k}(0) = \delta_{n,0} \hat{\xi}_k, \quad (21b)$$

$$\partial_y \hat{u}_{n,k}(-a) - |k| \tanh(|k|(h-a)) \hat{u}_{n,k}(-a) = \hat{J}_{n,k}(a), \quad (21c)$$

c.f. (13).

### 5.1. Numerical results: Transparent Boundary Condition

The problem (21) fits exactly into the framework outlined in Section 4 so that the Chebyshev tau and Legendre SEM approaches outlined there are available to us. As the depth of the *truncated* domain will be chosen quite small we anticipate that a small number of vertical discretization points will be required so that our original Chebyshev tau approach will be extremely fast and stable. In this section we focus upon this approach and study the limit as  $a \rightarrow |\sigma|_{L^\infty}$ .

In Tables 4 and 5 we report on results of a convergence study for the  $h = 1000, L = 2\pi$  DNO computation with exact solution discussed in Section 4.2. Again, we have selected the cosine profile,  $f(x) = \cos(x)$ , and begin with the rather small value of the perturbation parameter,  $\varepsilon = 0.01$ . As we see in Table 4, for  $a$  sufficiently large we can always find a value of  $N_y$  for which we can realize our target relative error tolerance  $10^{-10}$  (e.g.,  $N_y = 48$  when  $a = 10$ ,  $N_y = 24$  when  $a = 5$ , etc.). We also report on the errors we can realize with an extremely small number of Chebyshev coefficients,  $N_y = 8$ . Here we can only trust two digits of accuracy when  $a = 10$ , while we steadily gain improvement as  $a$  is decreased to  $1/2$ , where we realize errors of  $10^{-9}$ .

In Table 5 we study the effect of taking  $a$  even smaller, down to the point of cavitation (in the untransformed coordinates) and *beyond*. Here we see that, with only  $N_y = 8$  Chebyshev coefficients, we can compute solutions with relative error of  $10^{-12}$  for values of  $a$  all the way to  $a = \varepsilon = 0.01$ . Unsure of what this means theoretically, we continued our computations for values of  $a < \varepsilon$  and were shocked to learn that for values of  $a = 0.007, 0.006, 0.005$  we were still finding solutions accurate to  $10^{-11}$ , and passable solutions (errors of the order  $10^{-9}$ ) for  $a = 0.002$ , an amazing *one-fifth* the size of the deformation.

To test the robustness of this observation that the AB may be selected at the point of cavitation and beyond we have repeated the above computations in the more challenging cases  $\varepsilon = 0.1$  and  $\varepsilon = 0.5$ . For these configurations it was necessary to

**Table 4**

Numerical parameters, location of Artificial Boundary ( $y = -a$ ) and relative errors for Chebyshev tau simulation of the DNO with  $\varepsilon = 0.01, h = 1000$ , and  $L = 2\pi$ .

$N_x$	$N_y$	$E$	$N$	$a$	Relative error
32	8	1	4	10.0	0.0445198
32	48	1	4	10.0	$1.13526 \times 10^{-9}$
32	8	1	4	5.0	0.00303637
32	24	1	4	5.0	$4.22408 \times 10^{-12}$
32	8	1	4	2.0	$1.91894 \times 10^{-5}$
32	16	1	4	2.0	$4.10509 \times 10^{-12}$
32	8	1	4	1.0	$1.81372 \times 10^{-7}$
32	12	1	4	1.0	$5.03859 \times 10^{-12}$
32	8	1	4	0.5	$1.12494 \times 10^{-9}$
32	12	1	4	0.5	$4.11685 \times 10^{-12}$

**Table 5**

Numerical parameters, location of Artificial Boundary ( $y = -a$ ) and relative errors for Chebyshev tau simulation of the DNO with  $\varepsilon = 0.01$ ,  $h = 1000$ , and  $L = 2\pi$ .

$N_x$	$N_y$	$E$	$N$	$a$	Relative error
32	8	1	4	0.2	$4.62913 \times 10^{-12}$
32	8	1	4	0.1	$4.03905 \times 10^{-12}$
32	8	1	4	0.05	$4.08725 \times 10^{-12}$
32	8	1	4	0.02	$4.42811 \times 10^{-12}$
32	8	1	4	0.01	$5.58921 \times 10^{-12}$
32	8	1	4	0.007	$1.71914 \times 10^{-11}$
32	8	1	4	0.006	$1.99822 \times 10^{-11}$
32	8	1	4	0.005	$8.52513 \times 10^{-11}$
32	8	1	4	0.004	$2.58466 \times 10^{-10}$
32	8	1	4	0.003	$5.35013 \times 10^{-10}$
32	8	1	4	0.002	$4.31209 \times 10^{-9}$

**Table 6**

Numerical parameters, location of Artificial Boundary ( $y = -a$ ) and relative errors for Chebyshev tau simulation of the DNO with  $\varepsilon = 0.1$ ,  $h = 1000$ , and  $L = 2\pi$ .

$N_x$	$N_y$	$E$	$N$	$a$	Relative error
32	12	1	8	1.0	$3.81104 \times 10^{-11}$
32	12	1	8	0.5	$2.54616 \times 10^{-11}$
32	12	1	8	0.2	$2.52369 \times 10^{-11}$
32	12	1	8	0.1	$2.54207 \times 10^{-11}$
32	12	1	8	0.05	$7.25166 \times 10^{-10}$
32	12	1	8	0.04	$5.79425 \times 10^{-9}$

**Table 7**

Numerical parameters, location of Artificial Boundary ( $y = -a$ ) and relative errors for Chebyshev tau simulation of the DNO with  $\varepsilon = 0.5$ ,  $h = 1000$ , and  $L = 2\pi$ .

$N_x$	$N_y$	$E$	$N$	$a$	Relative error
32	18	1	28	2.0	$1.09205 \times 10^{-11}$
32	18	1	28	1.0	$7.88692 \times 10^{-12}$
32	18	1	28	0.7	$5.20779 \times 10^{-10}$
32	18	1	28	0.6	$1.69535 \times 10^{-8}$
32	18	1	48	0.6	$2.89295 \times 10^{-10}$
32	18	1	52	0.6	$1.29075 \times 10^{-10}$
32	18	1	52	0.5	$6.03476 \times 10^{-7}$
32	24	1	100	0.5	$2.37799 \times 10^{-7}$

take  $\{N_y = 12, N = 8\}$  and  $\{N_y = 18, N = 28\}$  for  $\varepsilon = 0.1$  and  $\varepsilon = 0.5$ , respectively. In Tables 6 and 7 we record results of our experiments as we took  $\varepsilon \rightarrow a$ . We see that in the case  $\varepsilon = 0.1$  we can still realize our target accuracy for choices of  $a$  in a neighborhood close to  $\varepsilon$ , however, we are unable to quite reach  $10^{-10}$  error for  $a \ll \varepsilon$ . The situation is even more restrictive when  $\varepsilon = 0.5$  where  $a = 0.6$  can be accommodated, however, an enormous number of Taylor terms must be retained  $N = 52$  before an acceptable error can be found. In the case  $a = \varepsilon$  we are unable to compute with an error less than  $10^{-7}$  even with 100 Taylor terms.

## 5.2. Other algorithms

At this point one can wonder about the possibility of computing DNO via other algorithms. Before commenting on this possibility let us gather some facts regarding the TFE approach gathered from the settled science on the subject [7–9,19,10,56,57]:

1. Boundary Perturbation Methods (BPM) take advantage of the analyticity properties of the problem unknowns with respect to shape deformations (parametrized, e.g., by the variable  $\varepsilon$ ) [7]. These properties are used to justify the *strongly* convergent Taylor series expansions of quantities of interest, e.g. (10), and guarantee that truncations of these will converge to the solution *exponentially quickly* within the disk of convergence of the Taylor series [57]. In this sense they are high-order/spectral (HOS) methods [48].
2. Regions of analyticity *outside* the disk of convergence of the Taylor series oftentimes exist. In fact, for DNO, it was shown in [9] that this region contains the *entire* real axis (up to geometric obstruction, i.e.  $|\varepsilon| < h$ ).

3. In infinite precision, with a suitable analytic continuation strategy, very large values of  $\varepsilon$  can be simulated. In fact, for DNO with  $h = \infty$ , any real value of  $\varepsilon$  is permitted.
4. In finite precision there are two obstacles which prevent convergence:
  - (a) Instabilities in *some* BPM algorithms: One important conclusion of the line of research [7–9] was that the classical BPM of “Field Expansions” (FE) and “Operator Expansions” (OE) require strong cancellations for their convergence. When a small number of Taylor orders are sufficient for a desired accuracy these effects are not noticed. However, when many orders are required (e.g.,  $\varepsilon$  is large and/or  $f$  is “rough”) this can be problematic and even *prevent* the attainment of a desired accuracy (see, e.g., the results of the simulation reported in Remark 1 in the case  $\varepsilon = 0.5$ ). The approach we advocate here, Transformed Field Expansions (TFE), *does not depend upon strong cancellations for its convergence*. In general, highly accurate estimates of very high order terms can be stably and accurately obtained. The only practical limitation to the size of  $\varepsilon$  is placed by the instabilities of the numerical analytic continuation procedure; see the next point.
  - (b) Instabilities in Padé approximation: Bruno and Reitich [42] showed that classical Padé approximation techniques are very ill-conditioned, while enhancements are difficult to construct and problem-specific.
5. As we commented in Remark 1, there are configurations of practical interest which are beyond the reach of classical BPM (e.g., OE and FE) but within the domain of applicability of our new method TFE. The cost of this new approach is a volumetric discretization which, as we have demonstrated in this contribution, can be significantly ameliorated.

Given that we must perform a volumetric discretization to achieve our target accuracy in certain configurations, one can ponder the possibility of abandoning BPM altogether and resorting to a more classical approach, e.g., Finite Difference (FD), Finite Volume (FV), Finite Element Methods (FEM), etc. For this comparison we point out that our implementation is a HOS method not only in perturbation parameter, but also in the spatial variables  $x$  (Fourier collocation) and  $y$  (Chebyshev tau or Legendre SEM). We now appeal to the extensive and well-known literature regarding the comparison between HOS methods and classical approaches such as FD, FV, and FEM, e.g. Gottlieb and Orszag [48], Fornberg [58] (Chapter 7); Boyd [59] (Chapter 1); Deville et al. [18]; and Hesthaven et al. [60].

For instance, Boyd [59] tells us:

1. “When many decimal places of accuracy are needed, the contest between pseudospectral algorithms and finite difference and finite element methods is not an even battle but a rout: pseudospectral methods win hands-down.”
2. “. . . even when only a crude accuracy of perhaps 5% is needed, the high order of pseudospectral methods makes it possible to obtain this modest error with about half as many degrees of freedom, . . . spectral methods. . . are memory-minimizing.”

We also point out two significant difficulties which would be encountered by a FD, FV or FEM implementation which our method handles in an elegant and high-order fashion:

1. Non-trivial geometry: The domain of definition of our problem is  $S_{h,\sigma}$  which is, obviously, quite irregular at the upper domain. Our TFE approach handles this irregularity by mapping the domain to the separable geometry  $S_{h,0}$ . Without a similar mapping the FD method would be greatly challenged to maintain any accuracy as structured gridpoints will fall *outside* of the domain of definition of the problem. A FEM can handle this type of geometry with curved elements, however, extreme care must be taken to implement these correctly to maintain an appropriate order of accuracy; a significant difficulty compared with the straightforward approach used here.
2. Transparent Boundary Condition: In order to be competitive with our TFE approach, any other volumetric method *must* be able to accommodate the artificial boundary at  $y = -a$  and implement the Transparent Boundary Condition, (20c), there

$$\partial_y v(x, -a) - T[v(x, -a)] = 0.$$

However, the operator  $T$  is a Fourier multiplier and cannot be implemented exactly in either the FD, FV or FEM frameworks. In fact a sizeable literature exists regarding the coupling of these transparent boundary conditions to FEM (see, e.g. [20–23,51,24,25,52,61,53,54]) and approximations of these (e.g. [50,62,63]). However, the implementations are complicated, expensive, and fraught with subtleties.

In order to provide some data to support the assertions made above regarding the superiority of our HOS approach, we implement our DNO solver using one of these standard volumetric solvers (Finite Differences) and compare. To give this solver every possible advantage we remove the two difficulties above (complications due to non-trivial geometries and the faithful implementation of the Transparent Boundary Condition) and simply consider (13). That is, a Fourier method is used in the  $x$ -discretization to handle the Transparent Boundary Condition, and a domain mapping coupled to a boundary perturbation approach is used to address the complex geometry. We now perform an approximation of the DNO ( $h = 0.01, \varepsilon = 0.001$ ) via two algorithms for solving the two-point boundary value problem (13): The Chebyshev tau method we have advocated above, and a standard centered second-order Finite Difference scheme. We once again set as our goal a relative error of  $10^{-10}$  and realized  $7.6 \times 10^{-11}$  with our Chebyshev tau solver using parameter values  $N_x = 32, N_y = 8, N = 4$ , in average (over 10 iterations) time  $T_C = 0.13$  s. By comparison, the second-order Finite Difference approach required  $N_x = 32, N_y = 800, N = 4$  to realize a relative error of  $9.94 \times 10^{-10}$  in averaged (over 10 iterations) time  $T_{FD} = 134.7$  s which is roughly

1000 times slower! While this is one randomly selected example, it does show the extremely advantageous properties of HOS methods (such as our TFE algorithm) within their domain of applicability.

## 6. Conclusions

In this paper we have shown how the stable and high-order Transformed Field Expansions method for the simulation of boundary value and free boundary problems can be significantly enhanced in the case of very large domains. For such problems the standard Chebyshev tau approach is quite wasteful as many discretization points are distributed far away from the domain surface where, in many applications of interest, there are exponentially small changes in the solution. We advocated two approaches to addressing this issue: exponentially distributed gridpoints, and Artificial Boundaries close to the domain surface coupled to Transparent Boundary Conditions. Each approach was shown to be vastly more efficient without any compromise in stability or accuracy.

## Acknowledgments

The author wishes to thank P. Fischer for his invaluable assistance in this project. Not only did he provide MATLAB scripts for the Legendre SEM, but he also shared his expertise and experience in making these algorithms run fast. Additionally, his textbook [18] is not only informative but also a pleasure to read.

DPN gratefully acknowledges support from the National Science Foundation through grant No. DMS-0810958, and the Department of Energy under Award No. DE-SC0001549.

Disclaimer: This report was prepared as an account of work sponsored by an agency of the United States Government. Neither the United States Government nor any agency thereof, nor any of their employees, make any warranty, express or implied, or assumes any legal liability or responsibility for the accuracy, completeness, or usefulness of any information, apparatus, product, or process disclosed, or represents that its use would not infringe privately owned rights. Reference herein to any specific commercial product, process, or service by trade name, trademark, manufacturer, or otherwise does not necessarily constitute or imply its endorsement, recommendation, or favoring by the United States Government or any agency thereof. The views and opinions of authors expressed herein do not necessarily state or reflect those of the United States Government or any agency thereof.

## References

- [1] H. Lamb, *Hydrodynamics*, sixth ed., Cambridge University Press, Cambridge, 1993.
- [2] C. Godrèche (Ed.), *Solids Far From Equilibrium*, Cambridge University Press, Cambridge, 1992.
- [3] R. Petit (Ed.), *Electromagnetic Theory of Gratings*, Springer-Verlag, Berlin, 1980.
- [4] D.M. Milder, An improved formalism for rough-surface scattering of acoustic and electromagnetic waves, in: *Proceedings of SPIE – The International Society for Optical Engineering* (San Diego, 1991), vol. 1558, Int. Soc. for Optical Engineering, Bellingham, WA, 1991, pp. 213–221.
- [5] W. Craig, C. Sulem, Numerical simulation of gravity waves, *J. Comput. Phys.* 108 (1993) 73–83.
- [6] O.P. Bruno, F. Reitich, Numerical solution of diffraction problems: a method of variation of boundaries, *J. Opt. Soc. Am. A* 10 (6) (1993) 1168–1175.
- [7] D.P. Nicholls, F. Reitich, A new approach to analyticity of Dirichlet–Neumann operators, *Proc. Roy. Soc. Edinburgh Sect. A* 131 (6) (2001) 1411–1433.
- [8] D.P. Nicholls, F. Reitich, Stability of high-order perturbative methods for the computation of Dirichlet–Neumann operators, *J. Comput. Phys.* 170 (1) (2001) 276–298.
- [9] D.P. Nicholls, F. Reitich, Analytic continuation of Dirichlet–Neumann operators, *Numer. Math.* 94 (1) (2003) 107–146.
- [10] D.P. Nicholls, F. Reitich, Shape deformations in rough surface scattering: improved algorithms, *J. Opt. Soc. Am. A* 21 (4) (2004) 606–621.
- [11] D.P. Nicholls, F. Reitich, Rapid, stable, high-order computation of traveling water waves in three dimensions, *Eur. J. Mech. B Fluids* 25 (4) (2006) 406–424.
- [12] D.P. Nicholls, J. Shen, A stable high-order method for two-dimensional bounded-obstacle scattering, *SIAM J. Sci. Comput.* 28 (4) (2006) 1398–1419.
- [13] Q. Fang, D.P. Nicholls, J. Shen, A stable high-order method for three-dimensional bounded-obstacle scattering, *J. Comput. Phys.* 224 (2) (2007) 1145–1169.
- [14] D.P. Nicholls, A rapid boundary perturbation algorithm for scattering by families of rough surfaces, *J. Comput. Phys.* 228 (9) (2009) 3405–3420.
- [15] D.P. Nicholls, J. Orville, A boundary perturbation method for electromagnetic scattering from families of doubly periodic gratings, *J. Sci. Comput.* 45 (1) (2010) 471–486.
- [16] Q. Fang, J. Shen, L.-L. Wang, An efficient and accurate spectral method for acoustic scattering in elliptic domains, *Numer. Math. Theory Methods Appl.* 2 (3) (2009) 258–274.
- [17] D. Xiu, J. Shen, Efficient stochastic Galerkin methods for random diffusion equations, *J. Comput. Phys.* 228 (2) (2009) 266–281.
- [18] M.O. Deville, P.F. Fischer, E.H. Mund, *High-order Methods for Incompressible Fluid Flow*, Cambridge Monographs on Applied and Computational Mathematics, vol. 9, Cambridge University Press, Cambridge, 2002.
- [19] D.P. Nicholls, F. Reitich, Shape deformations in rough surface scattering: cancellations, conditioning, and convergence, *J. Opt. Soc. Am. A* 21 (4) (2004) 590–605.
- [20] H.D. Han, X.N. Wu, Approximation of infinite boundary condition and its application to finite element methods, *J. Comput. Math.* 3 (2) (1985) 179–192.
- [21] J.B. Keller, D. Givoli, Exact nonreflecting boundary conditions, *J. Comput. Phys.* 82 (1) (1989) 172–192.
- [22] D. Givoli, Nonreflecting boundary conditions, *J. Comput. Phys.* 94 (1) (1991) 1–29.
- [23] D. Givoli, J.B. Keller, Special finite elements for use with high-order boundary conditions, *Comput. Methods Appl. Mech. Eng.* 119 (3–4) (1994) 199–213.
- [24] M.J. Grote, J.B. Keller, On nonreflecting boundary conditions, *J. Comput. Phys.* 122 (2) (1995) 231–243.
- [25] D. Givoli, Recent advances in the DtN FE method, *Arch. Comput. Methods Eng.* 6 (2) (1999) 71–116.
- [26] F. Ihlenburg, *Finite Element Analysis of Acoustic Scattering*, Springer-Verlag, New York, 1998.
- [27] V. Zakharov, Stability of periodic waves of finite amplitude on the surface of a deep fluid, *Journal of Applied Mechanics and Technical Physics* 9 (1968) 190–194.
- [28] O.A. Ladyzhenskaya, N.N. Ural'tseva, *Linear and Quasilinear Elliptic Equations*, Academic Press, New York, 1968.
- [29] L.C. Evans, *Partial Differential Equations*, American Mathematical Society, Providence, RI, 1998.

- [30] B.J. West, K.A. Brueckner, R.S. Janda, D.M. Milder, R.L. Milton, A new numerical method for surface hydrodynamics, *J. Geophys. Res.* 92 (1987) 11803–11824.
- [31] D.M. Milder, An improved formalism for wave scattering from rough surfaces, *J. Acoust. Soc. Am.* 89 (2) (1991) 529–541.
- [32] D.M. Milder, H.T. Sharp, Efficient computation of rough surface scattering, in: *Mathematical and Numerical Aspects of Wave Propagation Phenomena* (Strasbourg, 1991), SIAM, Philadelphia, PA, 1991, pp. 314–322.
- [33] D.M. Milder, H.T. Sharp, An improved formalism for rough surface scattering. ii: Numerical trials in three dimensions, *J. Acoust. Soc. Am.* 91 (5) (1992) 2620–2626.
- [34] P.J. Kaczkowski, E.I. Thorsos, Application of the operator expansion method to scattering from one-dimensional moderately rough Dirichlet random surfaces, *J. Acoust. Soc. Am.* 96 (2) (1994) 957–972.
- [35] D.M. Milder, Role of the admittance operator in rough-surface scattering, *J. Acoust. Soc. Am.* 100 (2) (1996) 759–768.
- [36] D.M. Milder, An improved formalism for electromagnetic scattering from a perfectly conducting rough surface, *Radio Sci.* 31 (6) (1996) 1369–1376.
- [37] W. Craig, U. Schanz, C. Sulem, The modulation regime of three-dimensional water waves and the Davey–Stewartson system, *Ann. Inst. Henri Poincaré* 14 (1997) 615–667.
- [38] D.P. Nicholls, Traveling water waves: Spectral continuation methods with parallel implementation, *J. Comput. Phys.* 143 (1) (1998) 224–240.
- [39] W. Craig, D.P. Nicholls, Traveling gravity water waves in two and three dimensions, *Eur. J. Mech. B Fluids* 21 (6) (2002) 615–641.
- [40] O.P. Bruno, F. Reitich, Numerical solution of diffraction problems: A method of variation of boundaries. II. Finitely conducting gratings, Padé approximants, and singularities, *J. Opt. Soc. Am. A* 10 (11) (1993) 2307–2316.
- [41] O.P. Bruno, F. Reitich, Numerical solution of diffraction problems: a method of variation of boundaries. III. Doubly periodic gratings, *J. Opt. Soc. Am. A* 10 (12) (1993) 2551–2562.
- [42] O.P. Bruno, F. Reitich, Approximation of analytic functions: a method of enhanced convergence, *Math. Comp.* 63 (207) (1994) 195–213.
- [43] O.P. Bruno, F. Reitich, Calculation of electromagnetic scattering via boundary variations and analytic continuation, *Appl. Comput. Electromagn. Soc. J.* 11 (1) (1996) 17–31.
- [44] O.P. Bruno, F. Reitich, Boundary-variation solutions for bounded-obstacle scattering problems in three dimensions, *J. Acoust. Soc. Am.* 104 (5) (1998) 2579–2583.
- [45] O.P. Bruno, F. Reitich, High-order Boundary Perturbation Methods, *Mathematical Modeling in Optical Science*, vol. 22, SIAM, Philadelphia, PA, 2001, pp. 71–109. *frontiers in Applied Mathematics Series*.
- [46] A.P. Calderón, Cauchy integrals on Lipschitz curves and related operators, *Proc. Nat. Acad. Sci. USA* 75 (1977) 1324–1327.
- [47] R. Coifman, Y. Meyer, Nonlinear harmonic analysis and analytic dependence, in: *Pseudodifferential Operators and Applications* (Notre Dame, Ind., 1984), Amer. Math. Soc., 1985, pp. 71–78.
- [48] D. Gottlieb, S.A. Orszag, *Numerical analysis of spectral methods: theory and applications*, Society for Industrial and Applied Mathematics, Philadelphia, PA, 1977. *CBMS-NSF Regional Conference Series in Applied Mathematics*, No. 26.
- [49] G.A. Baker Jr., P. Graves-Morris, *Padé Approximants*, second ed., Cambridge University Press, Cambridge, 1996.
- [50] K. Feng, Finite element method and natural boundary reduction, in: *Proceedings of the International Congress of Mathematicians*, vol. 1, 2 (Warsaw, 1983), PWN, Warsaw, 1984, pp. 1439–1453.
- [51] D. Givoli, *Numerical Methods for Problems in Infinite Domains*, *Studies in Applied Mechanics*, vol. 33, Elsevier Scientific Publishing Co., Amsterdam, 1992.
- [52] D.P. Nicholls, N. Nigam, Exact non-reflecting boundary conditions on general domains, *J. Comput. Phys.* 194 (1) (2004) 278–303.
- [53] L. Chindelevitch, D.P. Nicholls, N. Nigam, Error analysis and preconditioning for an enhanced DtN-FE algorithm for exterior scattering problems, *J. Comput. Appl. Math.* 204 (2007).
- [54] T.L. Binford, D.P. Nicholls, N. Nigam, T. Warburton, Exact non-reflecting boundary conditions on general domains and hp-finite elements, *J. Scientific Comput.* 39 (2) (2009) 265–292.
- [55] C. Fazioli, D.P. Nicholls, Parametric analyticity of functional variations of Dirichlet–Neumann operators, *Differ. Integ. Eqns.* 21 (5–6) (2008) 541–574.
- [56] B. Hu, D.P. Nicholls, The domain of analyticity of Dirichlet–Neumann operators, *Proc. Roy. Soc. Edinburgh A* 140 (2) (2010) 367–389.
- [57] D.P. Nicholls, J. Shen, A rigorous numerical analysis of the transformed field expansion method, *SIAM J. Numer. Anal.* 47 (4) (2009) 2708–2734.
- [58] B. Fornberg, *A Practical Guide to Pseudospectral Methods*, *Cambridge Monographs on Applied and Computational Mathematics*, vol. 1, Cambridge University Press, Cambridge, 1996.
- [59] J.P. Boyd, *Chebyshev and Fourier Spectral Methods*, second ed., Dover Publications Inc., Mineola, NY, 2001.
- [60] J.S. Hesthaven, S. Gottlieb, D. Gottlieb, *Spectral Methods for Time-dependent Problems*, *Cambridge Monographs on Applied and Computational Mathematics*, vol. 21, Cambridge University Press, Cambridge, 2007.
- [61] D.P. Nicholls, N. Nigam, Error analysis of a coupled finite element/DtN map algorithm on general domains, *Numer. Math.* 105 (2) (2006) 267–298.
- [62] A. Bayliss, M. Gunzburger, E. Turkel, Boundary conditions for the numerical solution of elliptic equations in exterior regions, *SIAM J. Appl. Math.* 42 (2) (1982) 430–451.
- [63] J.-P. Berenger, A perfectly matched layer for the absorption of electromagnetic waves, *J. Comput. Phys.* 114 (2) (1994) 185–200.